CrossMark

Transient characteristics and adaptive fault ride through control strategy of DFIGs considering voltage phase angle jump

Xinshou TIAN[1], Yongning CHI[1], Weisheng WANG[1],
Gengyin LI[2], Haiyan TANG[1], Zhen WANG[1]

MPCE

Abstract Wind power in China has experienced fast development in recent years. However, areas rich in wind power resources are often far away from loads centers, which leads to weak connection between wind turbines and power grid. When a grid fault occurs, new transient characteristics in weak grid integrated with doubly-fed induction generators (DFIGs) may present, such as voltage phase angle jump. Current control strategies for wind turbine with strong grid connection are hard to be adapted under weak gird connection. This paper explores the transient characteristics of DFIGs under voltage phase angle jump through analyzing the operation and control characteristics of DFIGs connected into weak grid when the voltage phase angle jumps. Fault ride through (FRT) control strategy of DFIGs based on adaptive phase-locked loop is proposed to adapt weak grid condition. The reference frame of the proposed strategy will be changed in real-time to track the operation condition of DFIGs according to the terminal voltage, and different phase tracking method is adopted during the grid fault. Field data analysis and time domain simulation are carried out. The results show that voltage phase angle jumps when a grid fault occurs, which weakens the FRT capability of DFIGs, and the proposed FRT control strategy can optimize transient characteristics of DFIGs, and improve the FRT capability of DFIGs.

Keywords DFIGs, Voltage phase angle jump, Transient characteristics, Adaptive FRT control strategy

✉ Xinshou TIAN
  tianxinshou@epri.sgcc.com.cn

  Yongning CHI
  chiyn@epri.sgcc.com.cn

  Weisheng WANG
  wangws@epri.sgcc.com.cn

  Gengyin LI
  ligy@ncepu.edu.cn

  Haiyan TANG
  tanghy@epri.sgcc.com.cn

  Zhen WANG
  wangzh@epri.sgcc.com.cn

[1] State Key Laboratory of Operation and Control of Renewable Energy & Storage Systems, China Electric Power Research Institute, Haidian District, Beijing 100192, China

[2] State Key Laboratory of Alternate Electrical Power System with Renewable Energy Sources, North China Electric Power University, Changping District, Beijing 102206, China

1 Introduction

The commercial development of wind turbines has increased continuously during the past 15 years, and the total installed capacity of wind power in China has reached 114.6 GW by the end of 2014 [1]. Centralized development and long-distance transmission are the outstanding characteristics of wind energy development in China. Most of the wind farms are located at the end of grid, which leads to a very weak connection between wind turbines and power grid. Grid disturbance will cause complex transient process of wind turbines [2]. Since DFIGs can not only greatly improve the energy conversion efficiency, and reduce mechanical stresses of the prime mover, but also improve control capability and stability of power system, it is one of the popular commercial wind turbines [3].

🙋 Springer

Due to the application of non-synchronous generator with power electronics devices such as converter, the voltage phase angle of DFIGs is not related to the rotor position like conventional synchronous generator dose, and the voltage phase angle jumps when a grid fault occurs in weak grid [4]. Additionally, the application of phase-locked loop (PLL) increases the difficulty of transient characteristics analysis and FRT control strategy design [5]. How to maintain the reliability and security of power grid is important to the power grid operation when large scale wind turbines are connected to weak grid [6, 7].

In order to enhance the transient stability of power system, the FRT has become basic requirements for wind power plants (WPPs) [8]. Many researches investigate the transient response characteristics and explore FRT control strategies of wind turbines. Power converter controller with transient voltage support capability and pitch angle control are adopted to ensure the FRT capability of DFIGs based wind turbines and to improve the transient voltage stability of grid-connected wind farm [3]. Promising methods based on crowbar protection circuit [9–11] or rotor excitation control have been developed [12, 13]. A switching control strategy is proposed to coordinate series-dynamic-resistor, dc-link chopper and crowbar [14]. Fault current characteristics of DFIGs are proposed through deriving analytical expressions of fault current. Some researches focus on the transient characteristics of wind turbines and their impacts on transient stability of power system [15, 16].

Fundamental voltage synchronous signal detection methods have been proposed to solve the phase-locked problem, such as resonant compensator [17], sinusoidal amplitude integrator method [18], model reference adaptive algorithm [19]. Six methods in calculating the phase-angle-jump for measured voltage dips in a three-phase system are proposed and compared [20]. A benchmarking of small-signal dynamics of PLLs is presented in [21]. The influence of voltage phase angle jump and generator parameters on the transient process are analyzed in [22]. Fault current characteristics of DFIGs considering voltage phase angle jump are analyzed in [23, 24], and phase angle compensation principle is proposed in [25]. The voltage phase angle jump mechanism and its influence factors in weak grid connection of DFIGs have been presented based on mathematical deduction [4]. However, the analysis of impact of voltage phase angle jump on the FRT control capability of DFIGs is insufficient, and the effective FRT control strategy of DFIGs considering voltage phase angle jump needs to be designed.

Due to the characteristics of terminal voltage phase angle jump of DFIGs in weak grid when a grid fault occurs, the applicability of traditional FRT control strategy of DFIGs is facing great challenges. The purpose of this paper is to reveal the transient characteristics of DFIGs

considering voltage phase angle jump and to propose a FRT control strategy of DFIGs so that to guarantee the safe operation of power grid with large scale DFIGs integration. The main work of this paper can be described as follows: Section 2 analyzes the transient characteristics of DFIGs considering voltage phase angle jump. A FRT control strategy of DFIGs based on adaptive PLL is proposed and its principle is given in Sect. 3. Section 4 carries out the experiments and discusses. In the end, conclusions are drawn in Sect. 5.

2 Analysis of transient characteristics of DFIGs considering voltage phase angle jump

When a grid fault occurs, the voltage drops to a relative low level until a protection device trips and the circuit breakers isolate the fault. During this period, the DFIGs connected to the same bus with the faulted feeder will experience a complex transient process, especially in weak grid with large scale DFIGs integration. This section aims to reveal the voltage phase angle jump mechanism when a grid fault occurs, and to evaluate the effectiveness of traditional control strategy of DFIGs under voltage phase angle jump.

2.1 Analysis of voltage phase angle jump under grid fault

In recent years, model and controller of variable speed wind turbines have been conducted regarding power system analysis. Fifth-order mathematical model of DFIGs can represent the complete dynamics behaviors of stator and rotor, and its effectiveness has been widely verified, and is widely used to analyze the transient process of DFIGs. The voltage and flux plural vector model of DFIGs in the dq rotating reference frame can be expressed as [4]:

$$\begin{cases} U_s = \dfrac{\mathrm{d}\psi_s}{\mathrm{d}t} + \mathrm{j}\omega_e\psi_s + R_sI_s \\ U_r = \dfrac{\mathrm{d}\psi_r}{\mathrm{d}t} + \mathrm{j}\omega\psi_r + R_rI_r \\ \psi_s = L_sI_s + L_mI_r \\ \psi_r = L_rI_r + L_mI_s \end{cases} \tag{1}$$

where U is the voltage; I is the current; ψ is the flux; R is the resistance; L is the inductance; ω_e is the synchronous angular velocity; ω is the slip angular velocity; subscript s is the stator component; subscript r is the rotor component; and subscript m is the mutual interaction component.

The voltage-divider model can be used to formulate the voltage sag conditions caused by three-phase short circuit fault in radial systems according to (1). The equivalent circuit of power grid connected with DFIGs is shown in Fig. 1 [4, 23].
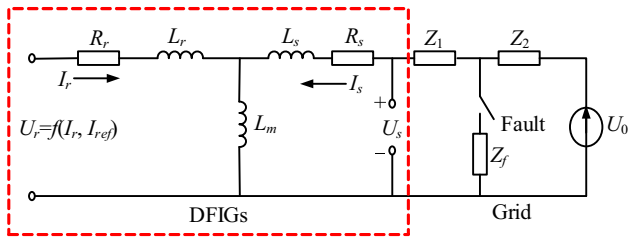
Fig. 1 Equivalent circuit of power grid connection of DFIGs

According to Fig. 1, the relation between voltage and current of power system in the steady-state condition can be defined as:

$$U_0 = U_{s0} + Z_0 I_{s0} \tag{2}$$

where U_0 is the external grid voltage; U_{s0} is the steady-state terminal voltage; I_{s0} is the steady-state stator current; and $Z_0 = Z_1 + Z_2$ is the impedance of transmission line.

It's assumed that the transient process of converter switch is ignored, and that the rotor current is equal to the reference value of rotor current. The voltage, current and flux vector of DFIGs are relative rest in the dq rotating reference frame, and the flux of generator is constant in the steady-state condition. The terminal voltage is determined by the external grid voltage and rotor current based on (1) and (2), which can be formulated as:

$$U_{s0} = \frac{Z_s}{Z_0 + Z_s} U_0 + \frac{jX_m Z_0}{Z_0 + Z_s} I_{r0} \tag{3}$$

where $Z_s = R_s + j\omega_e L_s$, $X_m = \omega_e L_m$, and I_{r0} is the steady-state rotor current.

Similarly, the structure of power system will change when a grid fault occurs in power grid in Fig. 1, and there will be a switch between normal operation control strategy and FRT control strategy of DFIGs. Then, the relation between voltage and current of power system under grid fault can be defined:

$$U_0 = \left(1 + \frac{Z_2}{Z_f}\right) U_{sf} + \left(Z_0 + \frac{Z_1 Z_2}{Z_f}\right) I_{sf} \tag{4}$$

where U_{sf} is the terminal fault voltage; I_{sf} is the stator fault current; and Z_f is the grounding resistance.

If ignore the transient process of stator and rotor, the terminal fault voltage is determined by the external grid voltage and rotor fault current based on (1) and (4), which can be formulated as:

$$U_{sf} = \frac{Z_f Z_s}{Z_f Z_s + Z_2 Z_s + Z_f Z_0 + Z_1 Z_2} U_0 + \frac{jX_m(Z_0 Z_f + Z_1 Z_2)}{Z_f Z_s + Z_2 Z_s + Z_f Z_0 + Z_1 Z_2} I_{rf} \tag{5}$$

where I_{rf} is the rotor fault current.

The three-phase short circuit fault will cause voltage magnitude drop as well as a sudden change of voltage phase angle in weak grid with large scale DFIGs integration. The phenomenon is referred to as "voltage phase angle jump". According to (1), (3) and (5), the change of terminal voltage is given by (6):

$$
\begin{aligned}
\Delta U_s &= U_{sf} - U_{s0} \\
&= \left(\frac{Z_f Z_s}{Z_f Z_s + Z_2 Z_s + Z_f Z_0 + Z_1 Z_2} - \frac{Z_s}{Z_0 + Z_s}\right) U_0 \\
&\quad + \frac{jX_m(Z_0 Z_f + Z_1 Z_2)}{Z_f Z_s + Z_2 Z_s + Z_f Z_0 + Z_1 Z_2} I_{rf} - \frac{jX_m Z_0}{Z_0 + Z_s} I_{r0}
\end{aligned}
\tag{6}
$$

Thus, the voltage phase angle jump value can be evaluated by (7) when a grid fault occurs.

$$\Delta \varphi = \arctan(\Delta U_s) \tag{7}$$

The value of voltage phase angle jump after the grid fault is close to the one when the grid fault occurs, which can be evaluated as:

$$\Delta \varphi' \approx -\Delta \varphi \tag{8}$$

The rotor current is equal to the reference value of rotor current ($I_{r0} = I_{ref0}$) in the steady-state condition, which can be evaluated as:

$$
\begin{cases}
I_{rd\_ref0} = -\dfrac{2P_{ref} L_s}{3U_s L_m} \\
I_{rq\_ref0} = \dfrac{2Q_{ref} L_s}{3U_s L_m} - \dfrac{U_s}{\omega_e L_m} \\
I_{ref0} = I_{rd\_ref0} + jI_{rq\_ref0}
\end{cases}
\tag{9}
$$

where P_{ref} is the reference value of active power; and Q_{ref} is the reference value of reactive power.

The rotor fault current is equal to reference value of rotor fault current ($I_{rf} = I_{ref1}$) when a grid fault occurs, I_{ref1} is the reference value of rotor fault current under FRT control strategy, which can be evaluated as follows [4].

$$
\begin{cases}
I_{rd\_ref1} = \lim\left(0, \sqrt{I_{max}^2 - I_{rq\_ref1}^2}\right) \\
I_{rq\_ref1} = -U_T/\omega_e L_m - K(0.9 - U_T)I_N L_s/L_m \\
I_{ref1} = I_{rd\_ref1} + jI_{rq\_ref1}
\end{cases}
\tag{10}
$$

where I_N is the rated current of DFIGs; U_T is the voltage of the point of common coupling (PCC); K is the dynamic reactive power compensation coefficient; and I_{max} is the maximum rotor current.

2.2 Response characteristics of PLL to voltage phase angle jump

PLL has been widely used for grid synchronization of power electronic converters. Generally speaking, PLL is a closed-loop dynamic system, where an internal oscillator is

controlled to keep in phase with the input periodic signal by means of a negative feedback loop. The structure of a typical PLL of DFIGs is shown in Fig. 2. It consists of three blocks: phase detector (PD), loop filter (LF), and voltage controlled oscillator (VCO).

The compensator $LF(s)$ is a proportional plus integral controller (*PI*), i.e. $LF(s) = k_p + k_i/s$, where k_p and k_i are the proportional and integral gains respectively, which is needed to meet the closed-loop performance specifications.

transfer function of phase angle error of voltage phase angle jump in Fig. 2 can be simply expressed as follows.

$$\theta_c^{\Delta\varphi}(s) = \frac{\Delta\varphi}{s}G(s) = \frac{2\zeta\omega_c s + \omega_c^2}{s(s^2 + 2\zeta\omega_c s + \omega_c^2)}\Delta\varphi \qquad (13)$$

The step response in frequency domain (13) can be transformed by Laplace inverse transformation into time domain in terms of tracking errors of the phase angle jump $\theta_c^{\Delta\varphi}(t)$, which is given by (14) [26].

$$\theta_c^{\Delta\varphi}(t) = \begin{cases} \left\{1 - e^{-\zeta\omega_c t}\left[\cos\left(\omega_c t\sqrt{1-\zeta^2}\right) - \dfrac{\zeta\sqrt{1-\zeta^2}}{1-\zeta^2}\sin\left(\omega_c t\sqrt{1-\zeta^2}\right)\right]\right\}\Delta\varphi & 0 < \zeta < 1 \\ (1 - e^{-\omega_c t} + \omega_c t e^{-\omega_c t})\Delta\varphi & \zeta = 1 \\ \left[1 - \dfrac{1}{2}\left(1 - \dfrac{\zeta\sqrt{\zeta^2-1}}{\zeta^2-1}\right)e^{-(\zeta-\sqrt{\zeta^2-1})\omega_c t} - \dfrac{1}{2}\left(1 + \dfrac{\zeta\sqrt{\zeta^2-1}}{\zeta^2-1}\right)e^{-(\zeta+\sqrt{\zeta^2-1})\omega_c t}\right]\Delta\varphi & \zeta > 1 \end{cases} \qquad (14)$$

The VCO function is represented as an integrator in Fig. 2. The open-loop transfer function of the PLL can be derived as:

$$G(s) = \frac{2\zeta\omega_c s + \omega_c^2}{s^2 + 2\zeta\omega_c s + \omega_c^2} \qquad (11)$$

where ω_c is the natural frequency, and ζ is the damping factor, which are given by:

$$\begin{cases} \omega_c = \sqrt{k_i} \\ \zeta = \dfrac{k_p}{2\sqrt{k_i}} \end{cases} \qquad (12)$$

The parameters of PLL, i.e. k_p and k_i can be determined by the values of ω_c and ζ. According to the stability requirements of power grid connection of large scale wind power based on PLL technology, the allowable variation range of ω_c and ζ can be obtained. The specific values of ω_c and ζ can be given based on actual demand. Terminal voltage phase angle jump $\Delta\varphi$ will occur under grid fault when large scale wind power based on DFIGs were connected into weak grid based on the above analysis. The
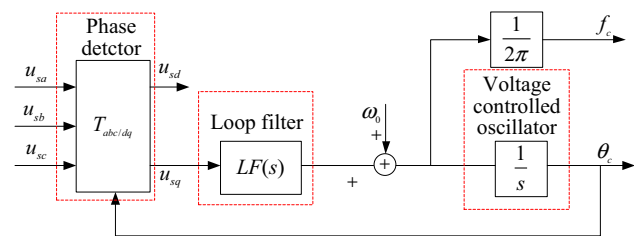
Figure 3 shows the response characteristics of PLL to the voltage phase angle jump in the condition of different parameters according to (14).

Figure 3 and (14) show that the higher natural frequency ω_c, the smaller damping factor ζ, and the faster transient response, the bigger overshoot. A high value of ω_c will decrease the disturbance rejection capability of the PLL, and the damping factor ζ has relatively less effect on the disturbance rejection ability of the PLL.

2.3 Impacts of voltage phase angle jump on the control capability of DFIGs

Figure 4 shows the relation between actual dq rotating reference frame and measured $d'q'$ rotating reference frame, which is determined by PLL technology when the terminal voltage orientation method is applied. There is a phase angle deviation θ_c between the two rotating reference frames when the voltage phase angle jumps.
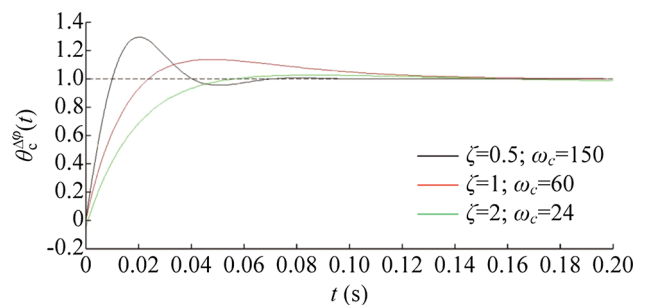

Fig. 2 The structure of a typical PLL of DFIGs

Fig. 3 Response characteristics of PLL to voltage phase angle jump

Fig. 4 Different reference frames

Fig. 5 Profile of power output of DFIGs caused by sudden increase of phase angle

Fig. 6 Profile of power output of DFIGs caused by sudden decrease of phase angle
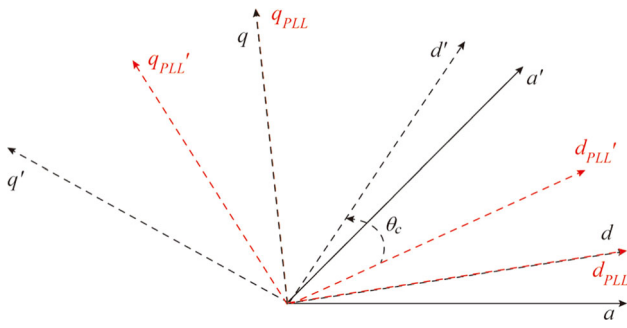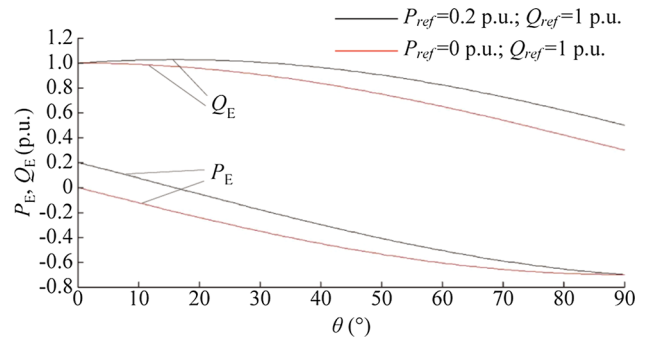
The phase angle deviation θ_c is shown in Fig. 4, the relation between the rotor current i_{rd} and i_{rq} based on dq rotating reference frame and the rotor current i'_{rd} and i'_{rq} based on $d'q'$ rotating reference frame can be expressed as:

$$\begin{bmatrix} i_{rd} \\ i_{rq} \end{bmatrix} == \begin{bmatrix} \cos\ \theta_c & \sin\ \theta_c \\ -\sin\ \theta_c & \cos\ \theta_c \end{bmatrix} \begin{bmatrix} i'_{rd} \\ i'_{rq} \end{bmatrix} \quad (15)$$

The decoupling control of active power and reactive power is failed due to the phase angle deviation θ_c. Then, the active power and reactive power output can be formulated by phase angle deviation θ_c, reference value of active power P_{ref} and reference value of reactive power Q_{ref}, respectively. According to (1), (9) and (15), the power output of DFIGs can be given by (16) if ignore the influence of control strategies and electromagnetic transient process of DFIGs.

$$\begin{cases} P_E = P_{ref}\cos\ \theta_c - \left(Q_{ref} - \dfrac{3}{2}\dfrac{U_S^2}{\omega_e L_s}\right)\sin\ \theta_c \\ Q_E = \dfrac{3}{2}\dfrac{U_S^2}{\omega_e L_s} + P_{ref}\sin\ \theta_c + \left(Q_{ref} - \dfrac{3}{2}\dfrac{U_S^2}{\omega_e L_s}\right)\cos\ \theta_c \end{cases}$$
$$(16)$$

Assume that the stator voltage orientation method of DFIGs is applied. Due to the application of PLL technology, there will be a phase angle deviation between the actual and measured rotating reference frame when the voltage phase angle jumps. The power output will be not equal to the power reference value any more, which decreases the control capability and transient stability of DFIGs. The power output characteristics of DFIGs can be illustrated in Fig. 5 based on (16) when there is a sudden increase of phase angle. Fig. 6 shows the power output characteristics of DFIGs when there is a sudden decrease of phase angle.

Figure 5 and Fig. 6 show that the bigger phase angle jump value, the larger power deviation between power output and power reference value when the phase angle deviation is within 0° to 90°. The maximum deviation of active power is up to 0.9 p.u., and the maximum deviation of reactive power is up to 0.4 p.u.. The control capability of DFIGs becomes poorer with the increasing of phase angle jump value.
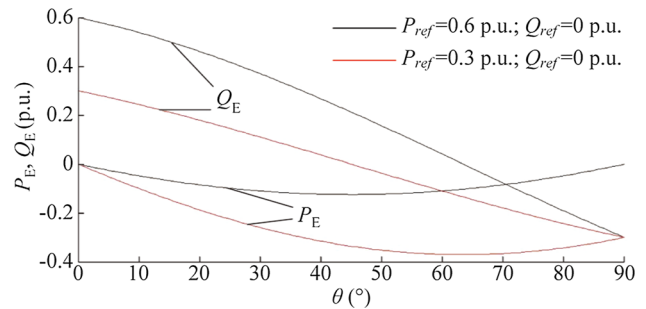
3 Adaptive FRT control strategy of DFIGs

3.1 FRT control strategy of DFIGs based on adaptive PLL

According to the above analysis, there is a voltage phase angle jump when a grid fault occurs or the grid fault is cleared in the condition of large scale of DFIGs connected to a weak grid, which weaken the control capability of DFIGs, and may cause FRT failure of DFIGs. In order to improve the controllability and transient stability of DFIGs under voltage phase angle jump, a FRT control strategy of DFIGs based on adaptive PLL is proposed in the paper, and its basic principle is presented in Fig. 7.

Figure 7 shows the basic principle of the proposed FRT control strategy. The strategy coordinates adaptive PLL and traditional FRT control used for stability control and post-fault stability control of fault process under voltage phase angle jump, and ensures FRT capability of variable speed wind turbines equipped with DFIGs. The different phase tracking method is adopted in different fault process. Stage 1: normal operation period, the voltage phase angle
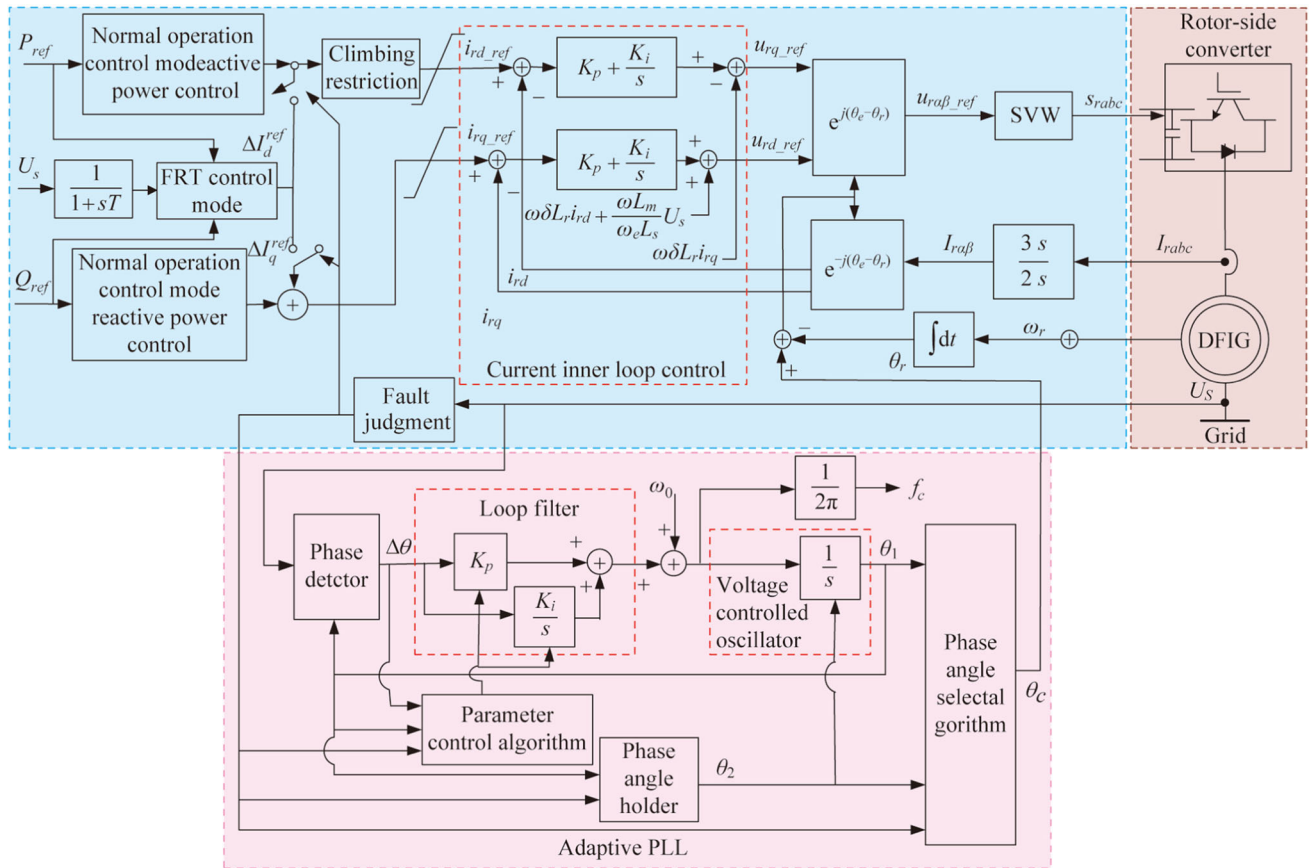
Fig. 7 Adaptive FRT control strategy of DFIGs

is constant in this period, and the traditional PLL shown in Fig 2. Stage 2: fault period, the phase tracking method based on locked phase angle is adopted as show in Fig. 7 during the grid fault. It can damp the change of voltage phase angle, so that to improve the stability and control capability of DFIGs. Stage 3: post-fault period, the phase tracking method based on variable parameter fast tracking is adopted as show in Fig. 7 after clearing the grid fault. The accuracy of phase tracking is guaranteed, and the stability and control capability of DFIGs are improved.

The detailed flow of FRT control strategy of DFIGs based on adaptive PLL is shown in Fig. 8.

The detailed flow of FRT control strategy of DFIGs based on adaptive PLL can be described as follows.

Step 1: Obtain the measured signal of terminal voltage U_s.

Step 2: Measure the range of terminal voltage U_s. Once the terminal voltage U_s is less than 0.9 p.u., DFIGs will transfer to FRT control mode, at the same time the phase angle holder module is activated, and the parameter control algorithm module is locked. The output phase angle of PLL θ_c will be equal to θ_{pre}, θ_{pre} is the terminal voltage phase angle before the grid fault. Then the next calculated cycle is carried out.
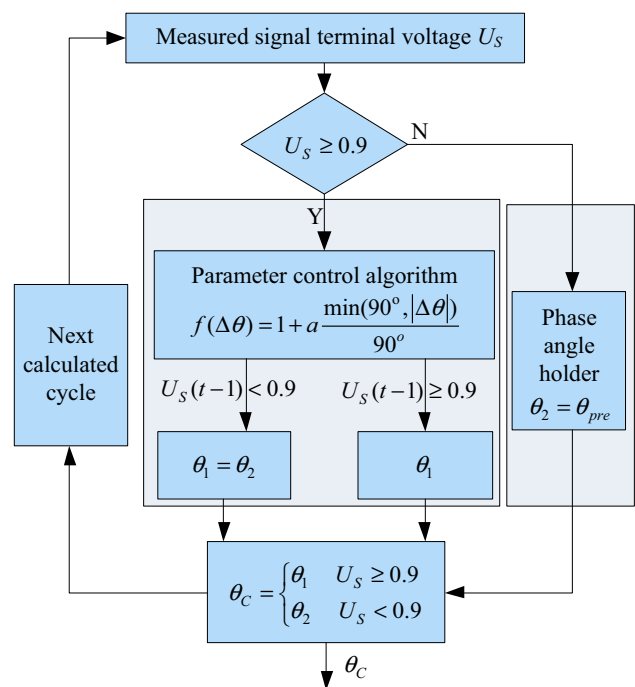

Fig. 8 Flow of FRT control strategy of DFIGs based on adaptive PLL

Step 3: If the terminal voltage U_s is up to 0.9 p.u., the parameter control algorithm module is activated. The parameter control function $f(\Delta\theta)$ is given by (17), and the parameters of PLL can be calculated by (18). Then, Step 4 is carried out.

$$f(\Delta\theta) = 1 + a\frac{\min(90^\circ, |\Delta\theta|)}{90^\circ} \tag{17}$$

where a is the phase angle deviation participation factor.

The parameter control function shows the degree of phase angle deviation $|\Delta\theta|$, which is within the range of 1 to $(1 + a)$. The bigger of phase angle deviation participation factor, the stronger capability of PLL to track phase angle change, and also the higher overshoot in phase angle tracking.

$$\begin{cases} \omega_c = f(\Delta\theta)\omega_{cN} \\ K_i = \omega_c^2 \\ K_p = 2\zeta\omega_c \end{cases} \tag{18}$$

where ω_{cN} is the reference natural frequency.

Step 4: Determine the control mode of DFIGs by judging whether it is the initial moment of voltage recovery control mode after clearing the grid fault. If the terminal voltage of previous calculated cycle $U_s(t-1)$ is less than 0.9 p.u., the DFIGs operates at the initial moment of voltage recovery control mode after clearing the grid fault, and the output phase angle of PLL θ_c will be equal to θ_2, otherwise θ_c will be equal to θ_1, then the next calculated cycle is carried out.

3.2 Stability analysis of adaptive FRT control strategy of DFIGs

The adaptive FRT control strategy has little impact on the operation of GSC of DFIGs. Firstly, only the voltage amplitude drops under the grid fault, while the voltage phase angle is stable. Moreover, the phase tracking of PLL is accurate. Therefore, the traditional control strategy of GSC can meet the requirements. Secondly, when the voltage phase angle jumps under the grid fault, the traditional control strategy of GSC has been adopted. There is a phase deviation between actual reference frame and measured reference frame given by tracking voltage phase through PLL. However, the operation effect of GSC is small, which can be neglected. The reasons can be summarized as: ① The converter capacity is smaller than that of DFIGs, thus there is a little impact of control strategy of GSC on power grid. ② The FRT control of DFIGs is implemented mainly through improving control strategy of RSC. Therefore the transient output characteristics of DFIGs are almost not affected by the control strategy of GSC. ③ The functions of control strategy of RSC are to keep the stability of DC capacitor voltage and to control

the reactive power exchange between GSC and power grid. The reactive power exchange is usually zero. At the same time, a slight fluctuation of DC capacitor voltage is allowed during the grid fault, and the chopper protection circuit can ensure the safety of DC capacitor.

The stability of power grid with large scale DFIGs will be approved when the adaptive FRT control strategy of DFIGs is adopted. Firstly, only the voltage amplitude drops under the grid fault, the control performance of DFIGs is identical under the traditional FRT control strategy and the adaptive FRT control strategy, and the operation stability of DFIGs can be guaranteed. Secondly, the voltage phase angle jump can be damped by the adaptive FRT control strategy when grid fault occurs. Thus the control capability of DFIGs is improved, and the transient characteristics of DFIGs are optimized. Then the operation stability of power grid with large scale DFIGs is improved.

4 Examples and analysis

In order to verify the accuracy and effectiveness of the proposed adaptive FRT control strategy in this paper, an example is provided using DIgSILENT/PowerFactory in this section. Figure 9 shows the structure diagram of study system, which includes one hundred 1.5 MW DFIGs. The parameters are obtained from an actual operation of DFIGs, i.e., $U_N = 690$ V, $R_s = 0.01$ p.u., $R_r = 0.01$ p.u., $L_s = 0.1$ p.u., $L_r = 0.1$ p.u., $L_m = 3.5$ p.u.. Wind farms are connected to an infinite power grid through a hundred kilometers of single circuit transmission line. The resistance of the line is 0.04 Ω/km, and the inductance of the line is 0.41 mH/km. The damping factor $\zeta = 0.707$, the reference natural frequency $\omega_{cN} = 120$, and the phase angle deviation participation factor of adaptive PLL $a = 4$. Suppose that the crowbar protection is inactivated, and the DFIGs is controlled during the grid fault.

4.1 Analysis of terminal voltage phase angle jump

The terminal voltage curves based on simulation, and field data of DFIGs are shown in Fig. 10 when the terminal
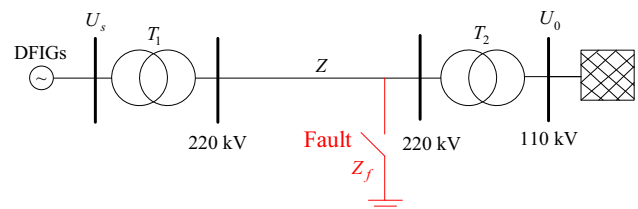

Fig. 9 Structure diagram of study system

voltage dropped to 0.2 p.u. and lasted for 625 ms. The field data of FRT are taken from a specific wind farm with 1.5 MW DFIGs based wind turbines. The simulation results are almost the same with the field data during the grid fault. The terminal voltage phase angle sudden increases when a grid fault occurs at 0.044 s, and sudden decreases when the grid fault is cleared at 0.669 s. The field data and simulation results demonstrate that the


(a) Terminal voltage curves during the grid fault

(b) Terminal voltage phase angle curves during the grid fault

(c) Terminal voltage curves when the grid fault occurs

(d) Terminal voltage curves when the grid fault is cleared

——— Field data; ——— Simulation results

Fig. 10 Simulation results and field data during FRT of DFIGs based wind turbine

terminal voltage phase angle jump is existed in the actual system when a grid fault occurs or the grid fault is cleared.

4.2 Analysis of transient characteristics of DFIGs under different FRT control strategy

It's assumed that a three-phase short circuit fault occurs on transmission line as shown in Fig. 9, and the grid fault is cleared after 120 ms. Two scenarios with different control strategies are designed to analyze the accuracy and effectiveness of the adaptive FRT control strategy of DFIGs. In the scenarios, the traditional FRT control strategy and adaptive FRT control strategy of DFIGs are implemented respectively. The comparison curves of terminal voltage amplitude, terminal voltage phase angle, active power output, reactive power output and rotor current are shown in Fig. 11.

As shown in Fig. 11, when a three-phase short circuit fault occurs and traditional FRT control strategy of DFIGs is adopted, the minimum drop of terminal voltage amplitude is 0.23 p.u.; the maximum jump of terminal voltage phase angle is 44.6°; the active power output of wind farm is 2.5 MW; the reactive power output of wind farm is 24 Mvar; and the maximum rotor surge current is 3.4 p.u.. While the minimum drop of terminal voltage amplitude is 0.33 p.u. when a three-phase short circuit fault occurs and the proposed adaptive FRT control strategy of DFIGs is adopted; the maximum jump of terminal voltage phase angle is 36.1°; the active power output of wind farms is 2.6 MW; the reactive power output of wind farms is 43 Mvar; and the maximum rotor surge current is 2.6 p.u..

When the three-phase short circuit fault is cleared, Figure 11 shows that the maximum jump of terminal voltage phase angle is 24°; the maximum absorbing reactive power of wind farm is 42 Mvar; and the maximum rotor surge current is 1.5 p.u. under the traditional FRT control strategy of DFIGs. While under the proposed adaptive FRT control strategy of DFIGs scenario, the maximum jump of terminal voltage phase angle is 7.1°; the maximum absorbing reactive power of wind farm is 24 Mvar; and the maximum rotor surge current is 1.1 p.u..
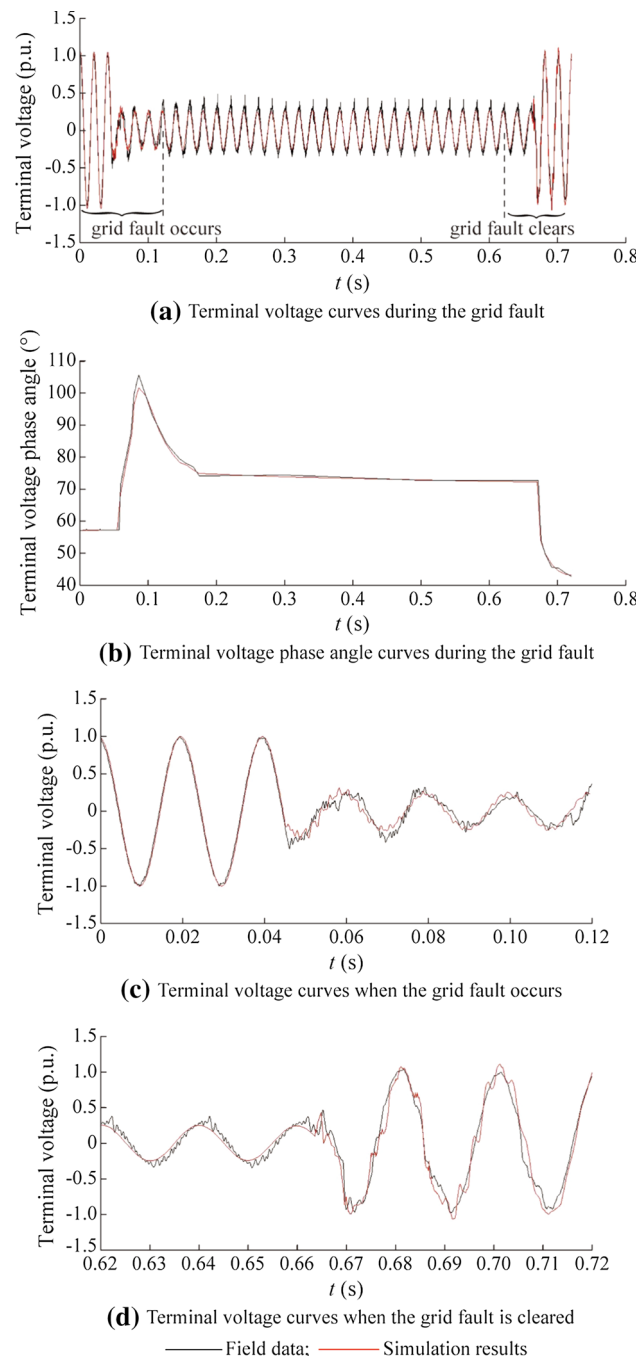
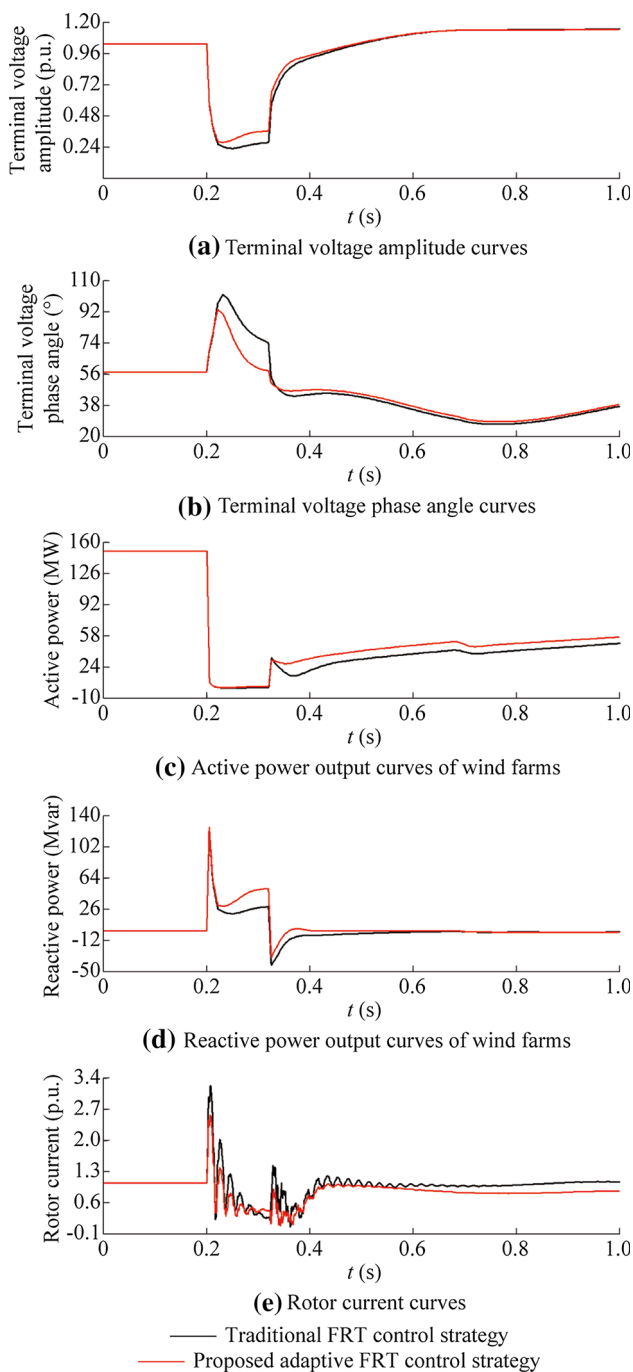## 5 Conclusion

The transient characteristics of DFIGs considering voltage phase angle jump has been analyzed, and a FRT control strategy of DFIGs based on adaptive PLL is proposed in this paper.

The following conclusions can be drawn through exploring the impacts of voltage phase angle jump on control capability of DFIGs, discussing the principle and

(a) Terminal voltage amplitude curves

(b) Terminal voltage phase angle curves

(c) Active power output curves of wind farms

(d) Reactive power output curves of wind farms

(e) Rotor current curves

—— Traditional FRT control strategy
—— Proposed adaptive FRT control strategy

Fig. 11 Transient characteristics of DFIGs under different FRT control strategy

stability of adaptive FRT control strategy, analyzing the field data and simulation results.

1) Terminal voltage phase angle jumps when a grid fault occurs or the grid fault is cleared in the condition of connecting large scale DFIGs into weak grid, and the current control strategies of wind turbines designed on an assumption of strong grid connection are hard to be adapted.

2) The locked phase angle is used to damp terminal voltage phase angle jump by the proposed adaptive FRT control strategy of DFIGs during the grid fault. It will decrease the terminal voltage amplitude drop, terminal voltage phase angle, maximum rotor current, and increase reactive power output.

3) The proposed adaptive FRT control strategy of DFIGs can track the change of terminal voltage, and transfer the operation state of PLL by dynamically distinguishing phase angle deviation to adapt system status after clearing the grid fault. It can decrease the terminal voltage phase angle jump value, the maximum rotor current and the maximum absorbing reactive power.

4) The proposed adaptive FRT control strategy can improve FRT capability of DFIGs considering voltage phase angle jump, and the transient characteristics of DFIGs are optimized.

References

[1] China installed wind power capacity 2014. Chinese Wind Energy Association, Beijing, China, 2015

[2] He YK, Hu JB (2012) Several hot-spot issues associated with the grid-connected operations of wind-turbine driven doubly fed induction generators. P CSEE 32(27):1–15

[3] Chi YN, Wang WS, Dai HZ (2007) Study on transient voltage stability enhancement of grid-connected wind farm with doubly fed induction generator installations. P CSEE 27(25):25–31

[4] Tian XS, Li GY, Chi YN et al (2016) Voltage phase angle jump characteristic of DFIGs in case of weak grid connection and grid fault. J Mod Power Syst Clean Energ 4(2):256–264. doi:10.1007/s40565-015-0180-4

[5] Göksu Ö, Teodorescu R, Bak CL et al (2014) Instability of wind turbine converters during current injection to low voltage grid faults and PLL frequency based stability solution. IEEE Trans Power Syst 29(4):1683–1691

[6] Zhou Y, Nguyen DD, Kjaer PC, et al (2013) Connecting wind power plant with weak grid-challenges and solutions. In: Proceedings of the IEEE power and energy society general meeting (PES'13), Vancouver, Canada, 21–25 Jul 2013, 7 pp

[7] Abulanwar S, Chen Z, Iov F (2013) Improved FRT control scheme for DFIG wind turbine connected to a weak grid. In: Proceedings of the 2013 IEEE PES Asia-Pacific power and energy engineering conference (APPEEC'13), Hong Kong, China, 8–11 Dec 2013, 6 pp

[8] Liu XG, Xu Z, Wong KP (2013) Recent advancement on technical requirements for grid integration of wind power. J Mod Power Syst Clean Energ 1(3):216–222. doi:10.1007/s40565-013-0036-9

[9] Morren J, de Haan SWH (2007) Short-circuit current of wind turbines with doubly fed induction generator. IEEE Trans Energ Conver 22(1):174–180

[10] Kong XP, Zhang Z, Yin XG et al (2015) Study of fault current characteristics of DFIG considering impact of crowbar protection. Trans China Electrotech Soc 30(8):1–10

[11] Sava GN, Duong MQ, Leva S, et al (2013) Coordination control of active crowbar for doubly fed induction generators. In: Proceedings of the 2014 international symposium on fundamentals of electrical engineering (ISFEE'14), Bucharest, Romania, 28–29 Nov 2014, 5 pp

[12] Rahimi M, Parniani M (2010) Grid-fault ride-through analysis and control of wind turbines with doubly fed induction generators. Electr Power Syst Res 80(2):184–195

[13] Lopez J, Sanchis P, Roboa X et al (2007) Dynamic behavior of the doubly fed induction generator during three-phase voltage dips. IEEE Trans Energy Conver 22(3):709–717

[14] Justo JJ, Mwasilu F, Jung JW (2014) Doubly fed induction generator wind turbines: A novel integrated protection circuit for low-voltage ride-through strategy. J Renew Sustain Energy 6(5):1560–1568

[15] Tian XS, Wang WS, Chi YN et al (2015) Performances of DFIG-based wind turbines during system fault and its impact on transient stability of power system. Automat Electr Power Syst 39(10):16–21. doi:10.7500/AEPS20140424006

[16] Vittal E, O'Malley M, Keane A (2012) Rotor angle stability with high penetrations of wind generation. IEEE Trans Power Syst 27(1):353–362

[17] Xu HL, Zhang W, Hu JB et al (2012) Synchronizing signal detection of fundamental voltage under unbalanced and/or distorted grid voltage condition. Automat Electr Power Syst 36(5):90–95

[18] Du X, Wang GN, Sun PJ et al (2013) Synchronization signal detection for grid fundamental voltage through employing sinusoidal amplitude integrators. P CSEE 33(36):104–111

[19] Pei XP, Hao XH, Chen W (2014) A novel three-phase phase-locked-loop system based on model reference adaptive algorithm. Trans China Electrotech Soc 29(4):196–204

[20] Wang Y, Bollen MJ, Xiao XY (2015) Calculation of the phase-angle-jump for voltage dips in three-phase systems. IEEE Trans Power Deliv 30(1):480–487

[21] Zhang C, Wang XF, Blaabjerg F, et al (2015) Benchmarking of small-signal dynamics of single-phase PLLs. In: Proceedings of the 9th international conference on power electronics and ECCE Asia (ICPE-ECCE Asia'15), Seoul, Republic of Korea, 1–5 Jun 2015, pp 1420–1427

[22] Mansour M, Islam S, Masoum MAS (2011) Impacts of symmetrical and asymmetrical voltage sags on DFIG-based wind turbines considering phase-angle jump, voltage recovery, and sag parameters. IEEE Trans Power Electron 26(5):1587–1598

[23] Xiong XF, Ouyang JX, Wen A (2012) An analysis on impacts and characteristics of voltage of DFIG-based wind turbine generator under grid short circuit. Automat Electr Power Syst 36(14):143–149

[24] Wang Y, Wu QW (2014) Electromagnetic transient response analysis of DFIG under cascading grid faults considering phase angel jumps. In: Proceedings of the 17th international conference on electrical machines and systems (ICEMS'14), Hangzhou, China, 22–25 Oct 2014, pp 1340–1344

[25] Wang W, Chen N, Zhu LZ et al (2009) Phase angle compensation control strategy for low-voltage ride through of doubly-fed induction generator. P CSEE 29(21):62–68

[26] Hu SS (2000) Automatic control theory. National Defence Industrial Press, Beijing, China

Xinshou TIAN received his B.E. degree from Huazhong University of Science and Technology, China, in 2008, M.E. degree from China Electric Power Research Institute, China, in 2011, and Ph.D. degree in electrical engineering from North China Electricity Power University, China, in 2016. Since 2016 he has been employed at China Electric Power Research Institute (CEPRI), Beijing, China. His main research interests include wind power generation and power system stability analysis.

Yongning CHI received his B.E. and M.E. degrees from Shandong University, China, in 1995, and 2002, respectively, and Ph.D. degree in electrical engineering from China Electric Power Research Institute, China, in 2006. Since 2003 he has been employed at China Electric Power Research Institute (CEPRI), Beijing, China, where he is the chief engineer (professor) for Renewable Energy Department. His research interests include modeling, control and integration analysis of renewable energy generation.

Weisheng WANG received his B.E. and M.E. degrees from Xi'an University of Technology, China, in 1990, and 1993, respectively, and Ph.D. degree in electrical engineering from Xi'an Jiaotong University, China, in 1996. Since 1997 he has been employed at China Electric Power Research Institute (CEPRI), Beijing, China, where he is the senior engineer (professor) and director of Renewable Energy Department of CEPRI. His research interest includes integration of renewable energy generation.

Gengyin LI received his B.S., M.S., and Ph.D. degrees from North China Electricity Power University, Beijing, China, in1984, 1987, and 1996, respectively, all in electrical engineering. Since1987, he has been with the School of Electrical and Electronic Engineering, North China Electricity Power University, Beijing, China, where he is currently a Professor and executive dean of the school. His research interests include power system analysis and control, HVDC and VSC-HVDC transmission technology.

Haiyan TANG received his B.E. and M.E. degrees from Hefei University of Technology, China, in 2000, and 2003, respectively, and Ph.D. degree in electrical engineering from China Electric Power Research Institute, China, in 2008. Since 2008 he has been employed at China Electric Power Research Institute (CEPRI), Beijing, China. His research interests include modeling, control and integration analysis of renewable energy generation.

Zhen WANG received Her B.E. degree and M.E. degree from North China Electric Power University in 2004 and 2007 respectively. Since 2007 She joined Renewable Energy Department of China Electric Power Research Institute in Beijing, China. Her main research interests include modeling and stability analysis of renewable energy generation.

STATE GRID
STATE GRID ELECTRIC POWER RESEARCH INSTITUTE